Commun Nonlinear Sci Numer Simulat 18 (2013) 1016–1026

Contents lists available at SciVerse ScienceDirect

Commun Nonlinear Sci Numer Simulat

journal homepage: www.elsevier.com/locate/cnsns

Parameter identification in periodic delay differential equations with distributed delay

Shahab Torkamani [a,*], Eric A. Butcher [a], Firas A. Khasawneh [b]

[a] Department of Mechanical and Aerospace Engineering, New Mexico State University, Las Cruces, NM 88003-8001, USA
[b] Department of Civil and Environmental Science, Duke University, Durham, NC 27708, USA

ARTICLE INFO

Article history:
Received 11 January 2012
Received in revised form 12 June 2012
Accepted 3 September 2012
Available online 12 September 2012

Keywords:
Integro-differential equations
Distributed delay
Parameter identification
Delay system

ABSTRACT

In this study, a parameter identification approach for identifying the parameters of a periodic delayed system with distributed delay is introduced based on time series analysis and spectral element analysis. Using this approach the parameters of the distributed delayed system can be identified from the time series of the response of the system. The experimental or numerical data of the response is examined with Floquet theory and time series analysis techniques to estimate a reduced order dynamics, or truncated state space to identify the Floquet multipliers. Parameter identification is then completed using a dynamic map developed for the assumed model of the system which can relate the Floquet multipliers to the unknown parameters in the model. The parameter identification technique is validated numerically for first and second order delay differential equations with distributed delay.

1. Introduction

Time-delayed dynamical systems, due to the vast variety of fields in science and engineering they can be relevant to, have attracted an increasing interest during past few decades. Some among their many practical applications are in areas such as manufacturing processes, robotics, neural networks, secure communication, traffic control, economics and biology [1–8]. For example cellular neural networks with delay coordinates may be considered as ideal models for neural networks which act using past knowledge, or as another example various parameters in the traffic control theory are also expressed in terms of delay coordinates. The primary complexity that introducing the delay adds to the system is the growth of the phase space from a finite dimension to an infinite dimension. However, it has been shown [9] that the behavior of the infinite dimension delayed system can be predicted using a finite dimension phase space. In fact, this approach makes use of transforming the original equations of the system to some sort of dynamic map that maps the system behavior over a single time delay.

When the effect of the past of a system is distributed over an interval, distributed delay terms appear in the system model. Modeling a system with a delay differential equation (DDE) having distributed delay, or as it is called in some references 'delayed integro-differential equations' (DIDE), is more complicated than that for a system with discrete delay. For instance, the force distribution on the interaction surface of the cutting edge of turning tool is represented by a distributed time delay model in [10,11]. In another example, when modeling the feeding system and the combustion chamber of a liquid fuel rocket motor, distributed time delay must be included to capture the non-steady flow with non-uniform lag [12]. Another instance where DIDEs appear in engineering is in studying the dynamics of wheel shimmy when the self-excited vibrations are related to the elasticity of the tire. If tire is modeled by a classical stretched string model, then the tire-ground contact patch

* Corresponding author. Tel.: +1 575 312 3365.
E-mail address: shahab@nmsu.edu (S. Torkamani).

1007-5704/$ - see front matter © 2012 Elsevier B.V. All rights reserved.
http://dx.doi.org/10.1016/j.cnsns.2012.09.001

is approximated by a contact line whose lateral deformation is given via a non-holonomic constraint. The mathematical form of this constraint is a partial differential equation which is coupled to an integro-differential equation governing the lateral motion of the wheel. By assuming travelling wave solutions for the deformation of the contact line, a DIDE appears in the problem [13].

Stability analysis of autonomous and time-periodic DIDEs has received some attention in the literature and several methods such as Runge–Kutta type methods [14,15], linear multi-step method along with Gauss quadrature [16], semi-discritization method [17,18], and quite recently spectral element analysis (SEA) method [19], have been developed to deal with stability problem of DIDEs. Other approaches to analyze the stability of constant and periodic DIDEs include the discretization of the infinitesimal generator of the solution operator [20–22], which can also be accomplished by using the Chebyshev spectral continuous time approximation (CSCTA ChSCTA) [23] to convert a time-periodic DIDE into a set of periodic ordinary differential equations (ODEs). The CSCTA ChSCTA formulation can be used for obtaining both the stability properties and time response of time-periodic DIDEs.

On the other hand, parameter estimation of linear time-periodic and nonlinear time-varying DDEs with constant delay have been studied, respectively, by Mann and Young [24] and by Deshmukh [25]. However, parameter identification of DIDEs has not yet received any attention in the literature. This paper extends the method used in [24] for parameter identification of linear periodic DDEs with discrete delay to a more general case of parameter identification in linear periodic DIDEs. To this end, first the experimental or numerical time series data is examined with empirical Floquet theory and principle orthogonal decomposition to estimate a reduced order dynamic. Then, the recently proposed method of spectral element analysis is used for discretization of an assumed DDE model with periodic coefficients and distributed delay and the original model is thus transformed into a form of dynamic map in terms of unknown parameters. Eventually, the Floquet multipliers of the reduced order dynamic of the time series are estimated and inserted in the dynamic map with unknown parameters. The unknown parameter of the assumed model is then identified through optimization of the parameters of characteristic equation using a least squares method.

In general, delays can be intrinsic to the model, e.g. machining processes, or they can be a modeling decision where we know that delays play a role in the system dynamics and therefore a delay is included in the system equation, e.g. epilepsy seizure models. When delays are intrinsic to the model, the mechanism by which the maximum delay enters the DIDE is understood and the magnitude of this delay is known. This case includes a large proportion of practical applications of DDE models and it is the case that this paper is primarily interested in. The current paper is organized as follows: The recently developed technique of spectral element analysis is employed in Section 2 to develop a dynamic map of the DIDE and it is described how this dynamic map can be made use of in a parameter identification procedure if the Floquet multipliers of the system are already estimated from the response. In Section 3 an approach based on nonlinear time series analysis is described that can estimate the Floquet multipliers from the time series of the response. In the next section a recently introduced technique is used to numerically integrate first and second order DIDEs prior to implementing the parameter identification approach in which various parameters of the time delay system are identified from the response.

2. Dynamic map formulation

As described previously, a DDE model with periodic coefficients and distributed delay is assumed for the experimental or numerical time series data and a discretization method needs to be used to develop a dynamic map. The discretization method that is used in this paper is the newly developed method of spectral element analysis (SEA). The primary reason for this preference is the faster rate of convergence that this method has compared to other extant methods [26,27]. What makes the SEA method a standout among other discretization techniques is that the SEA is a Galerkin-type method that discretizes the state space using a more accurate and more numerically stable interpolation formula on a well-conditioned set of mesh points. As a result of the smaller number of discretization points needed for convergence, this method reduces the symbolic manipulation volume required by our approach. The method of spectral element analysis is summarized from [19] in the rest of this section.

The form of the delayed integro-differential equation that is assumed in this paper is a linear DIDE with periodic coefficients, c.f.

$$\dot{x}(t) = \mathbf{A}(t)x(t) + \int_0^{v} \mathbf{K}(t,s)x(t-s)ds \tag{1}$$

where $\mathbf{K}(t,s)$ is a bounded kernel function, $v > 0$ is the duration of the bounded distributed delay and $\mathbf{K}(t,s)$ and $\mathbf{A}(t)$ are both periodic matrices, i.e. $\mathbf{A}(t) = \mathbf{A}(t+T)$, $\mathbf{K}(t,s) = \mathbf{K}(t+T,s)$. The first step in the analysis is to discretize the integral term in the DIDE. To this end, an mth order Gauss quadrature rule is applied to estimate the integral as

$$\int_0^{v} K(t,s)x(t-s)ds = \frac{v}{2}\sum_{k=1}^{m+1} w_k^* K(t,s_k)x(t-s_k) \tag{2}$$

where s_k and w_k^* are the Gauss nodes and weights, respectively. The Legendre–Gauss–Lobatto (LGL) points obtained from solving for the roots of

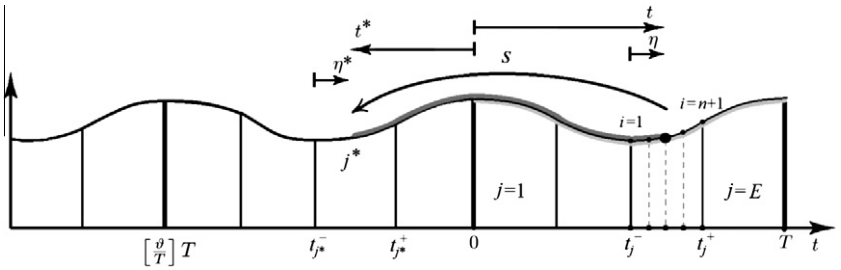

Fig. 1. Discretization of temporal elements and interpolation nodes within each element. Each point within element j at current interval (light gray), is mapped back to a set of $m+1$ delayed points at j^* elements of a delayed interval (dark gray) which can span over the current and previous periods.

$$(1-u^2)L'_m(u)=0 \tag{3}$$

are used as the Gauss nodes, where $L_m(u)$ is the Legendre polynomial of order m and the LGL points $u\in[-1,1]$ can be shifted to an arbitrary interval $\tilde{u}\in[a=0,b=v]$ through the relation $\tilde{u}=\frac{b-a}{2}u+\frac{b+2}{2}$. The corresponding quadrature weights are obtained using

$$w_k^*=\begin{cases}\frac{2}{m(m+1)} & k=1,m+1\\ \frac{2}{m(m+1)(L_m(t_k))^2} & \text{otherwise}\end{cases} \tag{4}$$

Since Eq. (2) yields an accurate approximation only if the integrand can be written as a polynomial of order $2m+1$, the number of the quadrature points in this paper is fixed to m and it is assumed that the integrands are well approximated by such polynomials.

In the next step, the interval $[0,T]$ is divided into E elements and a set of $n+1$ interpolation nodes is defined within each element as illustrated in Fig. 1. The length of each element j is defined as

$$h_j=t_j^+-t_j^- \tag{5}$$

where t_j^- and t_j^+ are the lower and higher endpoints of the element j as shown in Fig. 1. For simplicity, if the system is autonomous we can set $T=v$. Although any set of distinct points can be used as the interpolation points, due to the enhanced numerical stability of the approximation when using a set of points that are the roots or extrema of orthogonal functions, again the shifted LGL points are used as the interpolation nodes.

In spectral element method, the approximate solution for the jth element of the current period of the state is considered as a linear combination of polynomials or trial functions, ϕ_i, according to

$$x_j(t)=\sum_{i=1}^{n+1}X_{ji}\phi_i(\eta) \tag{6}$$

where $\eta\in[0,1]$ is the normalized local time within each element and X_{ji} are the undetermined coefficients of the current state. The trial functions in this paper are obtained using a representation of Lagrange polynomials provided by a barycentric formula which has a better numerical stability than the conventional Lagrange representation and is described as

$$\phi_i(\eta)=\frac{\frac{\bar{w}_i}{\eta-\eta_i}}{\sum_{k=1}^{n+1}\frac{\bar{w}_k}{\eta-\eta_k}} \tag{7}$$

where η_i and η_k are the ith and kth interpolation nodes, respectively and $\bar{w}_k$ are the barycentric weights defined as

$$\bar{w}_k=\frac{1}{\prod_{k\neq j}(\eta_j-\eta_k)}\quad j=1,\ldots,n+1 \tag{8}$$

The derivatives of the trial functions at the interpolation points can also be obtained using the same barycentric weights according to

$$\phi'_i(\eta_k)=\begin{cases}\frac{\bar{w}_i/\bar{w}_k}{\eta_i-\eta_k} & i\neq k\\ \sum_{i=0,i\neq k}^{n+1}-\frac{\bar{w}_i/\bar{w}_k}{\eta_i-\eta_k} & i=k\end{cases} \tag{9}$$

Substituting for the approximate solution from Eq. (6), the DIDE described by Eq. (1), after applying Gauss quadrature to the integral on the right hand side, yields

$$\sum_{i=1}^{n+1}\frac{1}{h_j}\dot{\phi}_i(\eta)X_{ji}-\mathbf{A}(\eta)\sum_{i=1}^{n+1}\phi_i(\eta)X_{ji}-\frac{v}{2}\sum_{k=1}^{m+1}w_k^*K(t_j^-+\eta h_j,s_k)\sum_{i=1}^{n+1}\phi_i(\eta_k^*)X_{j^*(t_k^*),i}^{q_k}=error \tag{10}$$

where η_k^* is the normalized delayed local time and $X_{j^*(t_k^*),i}^{q_k}$ are the undetermined coefficients of the delayed state. The nonzero residual error on the right side is due to the approximation procedure. The delayed time t_k^* is defined using modular arithmetic according to

$$t_k^*=t_j^-+\eta h_j-s_k(\mathrm{mod}\ T) \tag{11}$$

The normalized delayed local time can be obtained from

$$\eta_k^*=\frac{t_k^*-t_j^{*-}}{h_j^*} \tag{12}$$

where h_j^* and t_j^{*-} are respectively the length and the lower endpoint of the element the delayed time belongs to. Assuming the elements to have equal length, the element index to which the delayed time t_k^* belongs is given by

$$j^*(t_k^*)=\lceil t_k^*/h\rceil \tag{13}$$

where $\lceil\cdot\rceil$ represents the ceiling function. The number of period the delay looks back is specified by integer q_k which can be described by

$$q_k=\left|\left\lfloor\frac{t-s_k}{T}\right\rfloor\right| \tag{14}$$

where $\lfloor\cdot\rfloor$ represents the floor function. It is worth mentioning that for a DIDE any of the η_i interpolation points are mapped back onto a set of $m+1$ points due to the integral while $q_k=0$ indicates mapping onto the current period $[0,T]$.

In order to reduce the error in Eq. (10), the method of weighted residuals is used. To this end, the right side of the Eq. (10) is multiplied by a set of linearly independent weight functions $\psi_p(\eta)$, $p=1,\ldots,n$ and then integrated over the length of each element as

$$\int_0^1\left(\sum_{i=1}^{n+1}\frac{1}{h_j}\dot{\phi}_i(\eta)X_{ji}-\mathbf{A}(\eta)\sum_{i=1}^{n+1}\phi_i(\eta)X_{ji}-\frac{v}{2}\sum_{k=1}^{m+1}w_k^*K(t_j^-+\eta h_j,s_k)\sum_{i=1}^{n+1}\phi_i(\eta_k^*)X_{j^*(t_k^*),i}^{q_k}\right)\psi_p(\eta)d\eta=0 \tag{15}$$

The above integral can be approximated by the Gauss quadrature rule as in Eq. (2) having $N+1$ quadrature points η_r and weights w_r. Further simplification can be made by choosing the quadrature nodes to be the same as the interpolation nodes, namely $\{\eta_r\}_{r=1}^{N+1}=\{\eta_i\}_{i=1}^{n+1}$. Therefore, Eq. (15) yields,

$$\sum_{i=1}^{n+1}w_i\left(\sum_{i=1}^{n+1}\frac{1}{h_j}\dot{\phi}_i(\eta_i)X_{ji}-\mathbf{A}(\eta_i)\sum_{i=1}^{n+1}\phi_i(\eta_i)X_{ji}-\frac{v}{2}\sum_{k=1}^{m+1}w_k^*K(t_j^-+\eta_i h_j,s_k)\sum_{i=1}^{n+1}\phi_i(\eta_k^*)X_{j^*(t_k^*),i}^{q_k}\right)\psi_p(\eta_i)=0 \tag{16}$$

The above equation when expanded gives a set of $n+1$ algebraic equations of the states per each element that can be assembled into a global matrix form in terms of vectors of the current and delayed states described as

$$\mathbf{G}\mathbf{X}_n=\mathbf{H}\mathbf{X}_{n-1} \tag{17}$$

where $\mathbf{G}$ depicts the coefficients of the states in the interval $[T-v,T]$ while $\mathbf{H}$ represents the coefficients of the states in the interval $[-v,0]$. Consequently, the mapping from the states $\mathbf{X}_n\in[T-v,T]$ onto $\mathbf{X}_{n-1}\in[-v,0]$ is described by the dynamic map $X_n=\mathbf{Q}\mathbf{X}_{n-1}$ where $\mathbf{Q}=\mathbf{G}^{-1}\mathbf{H}$ is the monodromy matrix.

The eigenvalues of the monodromy matrix $\mathbf{Q}$ obtained through solving the characteristic equation are the Floquet multipliers of the system that can be used to determine the stability. In fact, the characteristic equation relates the Floquet multipliers to the parameters of the system. Therefore, if the Floquet multipliers of a system described by a DIDE model with an unknown parameter can somehow be estimated, then the dynamic map can be used to identify the unknown parameter as an implicit function of known Floquet multipliers.

3. Floquet multiplier estimation

In this section an approach is described based on time series analysis by developing a reduced order dynamics to estimate the Floquet multiplier of a time series. The time series data can be provided from experiments or generated numerically.

3.1. Reduced order dynamics

In this section, the stability of the system is inferred from a discrete dynamic map based on the fact that the stability of a periodic orbit of a system is closely related to the stability of the fixed point of the corresponding Poincare map. Consider a nonlinear system described by a dynamic map as

$$\mathbf{X}_{n+1} = \mathbf{g}(\mathbf{X}_n) \tag{18}$$

where $\mathbf{X}_n$ and $\mathbf{X}_{n+1}$ are $d \times 1$ state vectors and d is the dimension of the truncated system that will be discussed in the next subsection. The nonlinear terms on the right hand side can be expanded about a fixed point solution, $\mathbf{X}_f$, which yields,

$$\mathbf{X}_{n+1} = \mathbf{X}_f + \mathbf{P}(\mathbf{X}_n - \mathbf{X}_f) \tag{19}$$

where $\mathbf{P}$ is a $d \times d$ Jacobian matrix. The Poincare section can be constructed by picking samples of the time series of the system response at the frequency of the time delay. A Poincare map constructed from $\tilde{m}$ Poincare mappings can be formed in this way using the successive periodic samples, as

$$\mathbf{U} = \mathbf{PV} \tag{20}$$

where the matrices $\mathbf{U}$ and $\mathbf{V}$ are of dimension $d \times \tilde{m}$ and the elements of these matrices are given by

$$\begin{aligned} \mathbf{U} &= [\mathbf{X}_1\mathbf{X}_2 \ldots \mathbf{X}_{\tilde{m}+1}] - \mathbf{X}_f \\ \mathbf{V} &= [\mathbf{X}_0\mathbf{X}_1 \ldots \mathbf{X}_{\tilde{m}}] - \mathbf{X}_f \end{aligned} \tag{21}$$

The above $\mathbf{P}$ matrix is comparable with the monodromy matrix $\mathbf{Q}$ in previous section and the eigenvalues of this matrix obtained from solving a characteristic equation of order d can be considered as estimates of the Floquet multipliers of the system.

$$\hat{\mu}_i \cong eig(\mathbf{P}) \tag{22}$$

Although a minimum choice for the required number of Poincare points is $\tilde{m} = d$, it has been shown [28] that better estimates can be obtained for the over-constrained case ($\tilde{m} > d$). In this case, the expression for $\mathbf{P}$ can be found from a least squares method as

$$\mathbf{P} = \mathbf{UV}^T(\mathbf{VV}^T)^{-1} \tag{23}$$

The improved estimate of the least-square method can be explained as a result of a reduced experimental noise or numerical imprecision.

3.2. Reduced order model parameters

If the time series is the data measured in an experiment, then most likely the practitioner is only able to measure a single component of the state vector and the additional states of the system need to be determined somehow. Moreover, the dimension of the reduced order is still left to be determined. A technique commonly used in nonlinear time series analysis that can deal with both issues is to qualitatively reconstruct the attractor using a delay reconstruction approach [29].

It has been shown that taking delayed versions of this measured coordinate can, with an appropriately chosen delay, qualitatively preserve the dynamics of the unobserved variables. This means that a single measurement $x(n)$ can be used to reconstruct the k-dimensional state-space as,

$$\mathbf{x}(n) = \begin{Bmatrix} x(n) \\ x(n+\tau) \\ \vdots \\ x(n+(k-1)\tau) \end{Bmatrix} \tag{24}$$

where the delayed copies of $x(n)$ are often referred to as the pseudo-state vectors. A successful reconstruction requires the choice of both embedding delay τ and embedding dimension k. Two of the most widely acknowledged methods for choosing the proper delay and proper dimension in attractor reconstruction are average mutual information function [30] and false nearest neighbors [31], respectively.

Yet another approach for choosing system dimension based on singular value decomposition can be described as follows. The d-dimensional delayed state vector is initially embedded with equally spaced displacement data points over the time interval T. Each state is filled with Poincare points over $\tilde{m}$ periods, where $\tilde{m}$ is considered to be much larger than d. Then the rank of $\mathbf{VV}^T$ matrix is constantly computed while increasing the dimension of the state vector. The dimension at which the rank of the matrix stops growing demonstrates the proper system dimension.

4. Parameter identification and verification

In order to implement the described parameter identification approach, a numerical time series data of a DIDE system is needed. In Matlab, there are different built-in functions to integrate different types of DDEs, e.g. DDEs with multiple discrete delays and DDEs with state-dependent delay. However, a Matlab function capable of integrating a DIDE has not yet been developed. Therefore, an approach developed in [23] based on Chebyshev spectral continuous time approximation is used to integrate DIDEs in Matlab. The parameter identification approach is implemented in this paper on different time series

generated through integrating two types of first and second order periodic DIDEs using the aforementioned technique in Matlab.

The numerically generated response of the system is analyzed using time series analysis techniques to obtain the parameters needed for delay reconstruction. The V and U vectors are formed from Poincare mappings using Eq. (21), and then Eq. (23) yields the **P** matrix. The estimates of the Floquet multipliers $\hat{\mu}_i$ can be obtained using Eq. (22). On the other hand, as seen in Section 2 spectral element analysis can be used to determine the monodromy matrix of a DIDE. Therefore, the characteristic equation obtained from the SEA method can be employed to relate the Floquet multipliers to the unknown parameter of the system. If the SEA method with a single element and an equal number of quadrature and interpolation points ($n = m$) is applied on the DIDE of the system with an unknown parameter of Λ, then the resulting characteristic equation describes,

$$\mu^{n+1} + C_n(\Lambda)\mu^n + C_{n-1}(\Lambda)\mu^{n-1} + \ldots + C_0(\Lambda) = 0 \tag{25}$$

where μ is the characteristic multiplier and $C_i(\Lambda)$ is a ith order polynomial in terms of Λ. If we substitute for μ from the estimates of the Floquet multipliers $\hat{\mu}_i$ obtained from the reduced order map of the system, then the equation above can be solved for the unknown parameter Λ.

4.1. First order periodic DIDE

Consider the first order periodic DIDE described as

$$\dot{x}(t) = (\delta + \in cos\omega t)x(t) + \int_0^v K(t,s)x(t-s)ds \tag{26}$$

The stability charts of the above system with a kernel function of $K(t,s) = \beta$, for a periodic case ($\epsilon \neq 0$) is shown in Fig. 2. Note that the maximum limit of the distributed delay integral in this study is equal to the parametric forcing period, i.e. $v = \frac{2\pi}{\omega}$. To implement the parameter identification technique described in this study, the first order periodic DIDE of Eq. (26) with the following set of arbitrary parameters is considered:

$$K(t,s) = \beta, \quad \omega = 2\pi, \quad v = 1, \quad \epsilon = 5, \quad \delta = -0.45$$

Parameter β is assumed to be the unknown parameter of the system which is intended to be identified from the time series of the response, which is generated numerically by fixing a value for parameter β and then integrating the DIDE of the system. In order to study the parameter identification in both stable and unstable cases, two different values of $\beta = -2.1$ for the stable case (depicted by cross in Fig. 2) and $\beta = -2.6$ for the unstable case (depicted by star in Fig. 2) based on the stability chart of Fig. 2 are considered. The DIDE of the system is integrated in Matlab using the technique mentioned in the beginning of this section to generate the time history of the response. The time history of the response of the system with a sampling frequency of 40 Hz for both stable ($\beta = -2.1$) and unstable ($\beta = -2.6$) cases are demonstrated in Fig. 3.

The false nearest neighbor method and the mutual information function are then applied to the time series to obtain the parameters needed for delay reconstruction. The embedding dimensions of stable and unstable time series which determines the dimension of the reduced order dynamics are $\tilde{m} = 2$ and $\tilde{m} = 3$, respectively. Note that the time series data is scalar ($d = 1$) and $\tilde{m} > d$. The V and U vectors are then formed from Poincare mappings using Eq. (21) and noting that the fixed points $\mathbf{X}_f$ of the stable and unstable systems are both the origin. The **P** matrices obtained from Eq. (23) for both the stable and unstable cases are scalars. Therefore the estimated Floquet multipliers for the stable and unstable cases are $\hat{\mu} = -0.9399$ and

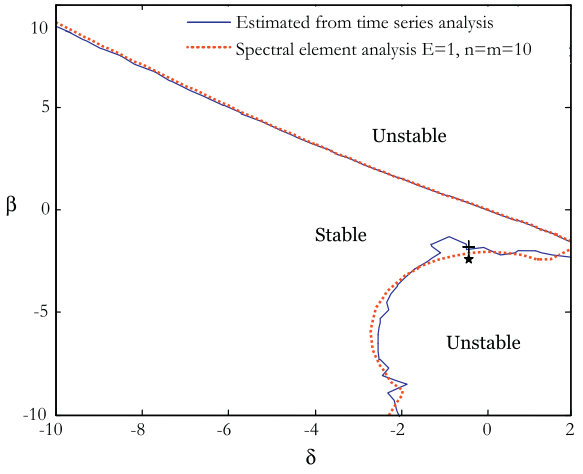

Fig. 2. Stability chart of the first order DIDE of Eq. (26) for periodic case of $\epsilon = 5$, $\omega = 2\pi$, $v = 1$, $K(t,s) = \beta$.

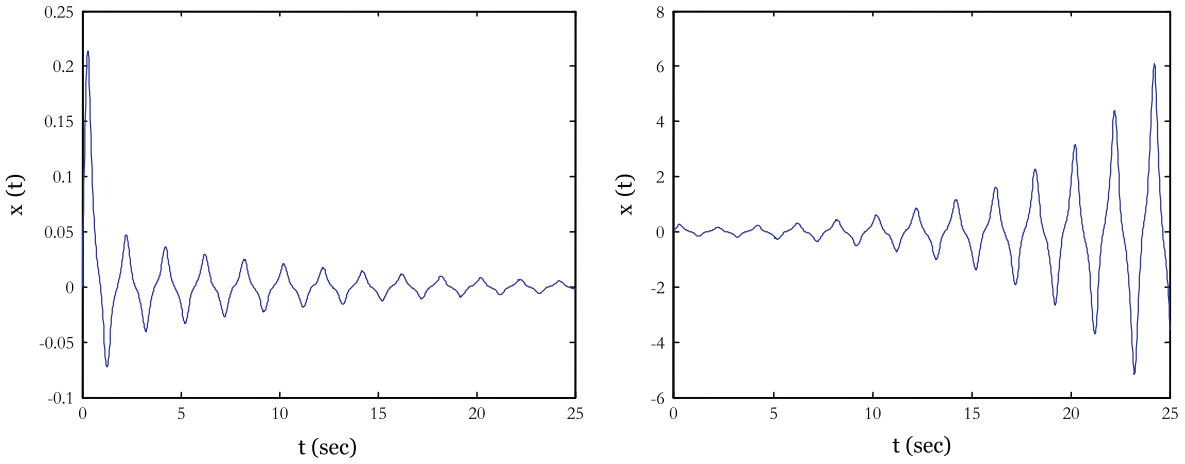

Fig. 3. Time history of the first order DIDE of Eq. (26) for a stable case of $\beta = -2.1$ (on the left) and unstable case of $\beta = -2.6$ (on the right). $\omega = 2\pi, \nu = 1, \epsilon = 5, \delta = -0.45$.

Table 1
The convergence study of the Floquet multiplier obtained from the SEA technique.

Number of elements	Number of interpolation/quadrature points	$\beta = -2.1$	$\beta = -2.6$
$E = 1$	$n = m = 2$	1.85	2.15
	$n = m = 3$	0.82	1.16
	$n = m = 4$	1.04	1.36
	$n = m = 5$	0.95	1.28
	$n = m = 6$	1.00	1.33
	$n = m = 7$	0.98	1.32
	$n = m = 8$	0.98	1.32
	$n = m = 9$	0.98	1.32
	$n = m = 10$	0.98	1.32

$\hat{\mu} = -1.2080$, respectively. The Floquet multipliers obtained by the SEA technique respectively are $\mu = -0.9841$ and $\mu = -1.3252$. This conveys the adequate accuracy of the Floquet multipliers estimated from the time series. The convergence study of the SEA technique in this case is shown in Table 1.

The characteristic equation obtained from the SEA method can be employed to relate the Floquet multipliers to the parameters of the system. If the SEA method with a single element and 7 interpolation points ($n = m = 7$) is applied on the DIDE of Eq. (26) with the known parameters mentioned before and an unknown parameter of β, it describes a characteristic equation in the form of Eq. (25) where $C_{i=1,\ldots,7}(\beta)$ are ith order polynomials in terms of β. Eventually by substituting for μ from the estimated Floquet multipliers (say $\hat{\mu} = -0.9399$), the final 7th order polynomial equation becomes

$$\beta^7 + a_1\beta^6 + a_2\beta^5 + a_3\beta^4 + a_4\beta^3 + a_5\beta^2 + a_6\beta + a_7 = 0 \tag{27}$$

where the a_i coefficients are listed in Appendix Table A-4. By solving the above equation for β the unknown parameter of the system can be identified as $\beta = -2.086$. Using the SEA method with one element and 7 interpolation points and using a similar procedure, the value of parameter β for the unstable time series of Fig. 3 will be $\beta = -2.480$. The identified parameters along with respective percentage of error are tabulated in Table 2.

The parameter identification approach is once again applied to the first order DIDE of Eq. (26) with the known parameters

$$K(t,s) = \beta, \quad \omega = 2\pi, \quad \nu = 1, \quad \epsilon = 5, \quad \beta = 0.1$$

and parameter δ as the unknown parameter. The values of parameter δ identified using a similar approach are listed in Table 2 along with the percentage of error. The results from Table 2 signify the capability of the approach in identification of the system parameters with a good accuracy.

Moreover, in order to better verify the procedure of Floquet multiplier estimation required in this parameter identification approach, the absolute value of the dominant Floquet multiplier estimated from the time series analysis procedure is compared for a wide range of time series generated through integrating the DIDE of Eq. (26) with different values of parameters δ and β. The absolute value of Floquet multiplier estimated from time series generated with different values of β or δ is compared with the Floquet multiplier obtained using the SEA method with 1 element and 10 interpolation points. The results of this comparison are depicted in Fig. 4. As seen from the figure, the Floquet multipliers estimated from time series are

Table 2
The estimated Floquet multiplier along with the actual and identified parameters of the system.

Parameter to be identified	Estimated $\hat{\mu}$	Identified value	Actual value	Error (%)
β	−0.9399	−2.086	−2.1	0.67
	−1.208	−2.480	−2.6	4.6
δ	2.950	0.981	1.0	1.8
	6.571	1.815	1.8	0.8

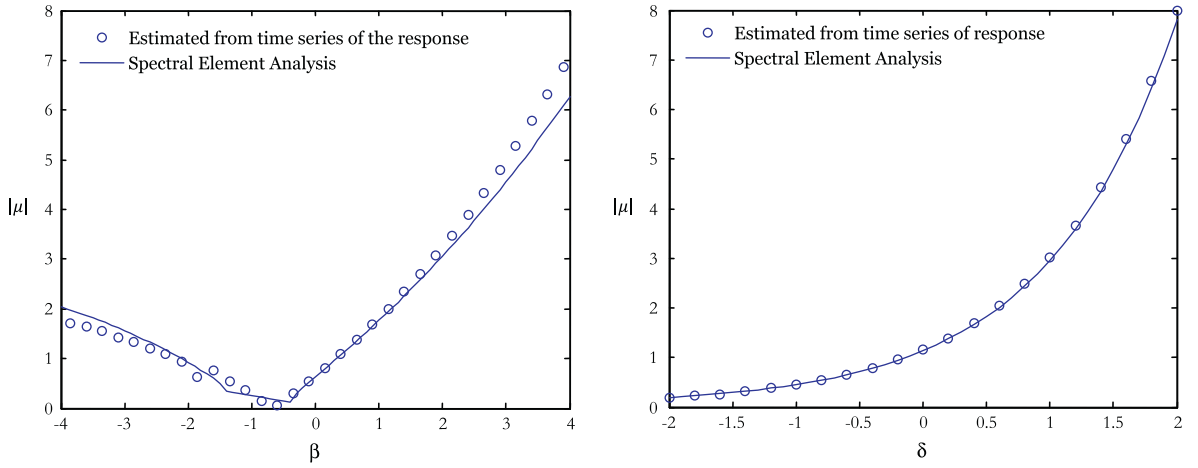

Fig. 4. Floquet multipliers estimated from time series of the response compared with the values obtained from SEA method: for $K(t,s) = \beta$, $\omega = 2\pi$, $v = 1$, $\epsilon = 5$, $\delta = -0.45$ and a varying β (left). Also for $K(t,s) = \beta$, $\omega = 2\pi$, $v = 1$, $\epsilon = 5$, $\beta = 0.1$ and a varying δ (right).

accurate enough to be used in the parameter identification approach. The stability chart of the system for a variety of parameter δ versus β estimated from time series using the procedure described in Section 3 compared with the stability chart obtained using the SEA method with 1 element and 10 interpolation points in Fig. 2, shows a good agreement.

4.2. Second order periodic DIDE

Now consider second order Mathieu type delay differential equation

$$\ddot{x}(t) + (\delta + \epsilon cos\omega t)x(t) = \int_0^v K(t,s)x(t-s)ds \tag{28}$$

which can be expressed in state space form of Eq. (1) with the $\mathbf{A}(t)$ and $\mathbf{K}(t,s)$ matrices as

$$\mathbf{A}(t) = \begin{bmatrix} 0 & 1 \\ -(\delta + \epsilon Cos\omega t) & 0 \end{bmatrix}, \quad \mathbf{K}(t,s) = \begin{bmatrix} 0 & 0 \\ K(t,s) & 0 \end{bmatrix} \tag{29}$$

The stability chart of the DIDE of Eq. (28) with a kernel function of $K(t,s) = \beta$ for a periodic case ($\epsilon = 5$) that is developed using SEA method using 2 elements and 10 interpolation points is depicted in Fig. 5.

The parameter identification approach is applied to the second order DIDE of Eq. (28) with the known parameters below

$$K(t,s) = \beta, \quad \omega = 2\pi, \quad v = 1, \quad \epsilon = 5, \quad \delta = 1.5$$

and the unknown parameter of β. The absolute value of the dominant Floquet multiplier for the above parameters and a wide range of parameter β estimated from numerically generated time series using the time series analysis procedure is depicted and compared with the results of SEA method in Fig. 6. The values of parameter β identified using the identification approach are listed in Table 3 along with the percentage of error.

Also the parameter identification approach is applied on the DIDE of Eq.(28) with the known parameters below and this time the unknown parameter δ.

$$K(t,s) = \beta, \quad \omega = 2\pi, \quad v = 1, \quad \epsilon = 5, \quad \beta = 0.8$$

The absolute values of the largest Floquet multiplier estimated from numerically generated time series is depicted and compared with the results of SEA method in Fig. 6 for a wide range of parameter δ. The values of parameter δ identified using the

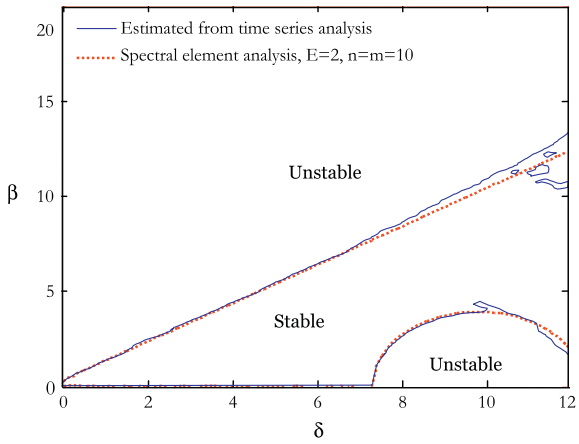

Fig. 5. Stability chart of the second order DIDE of Eq. (28) for periodic case of $\epsilon = 5$, $\omega = 2\pi$, $\nu = 1$, $K(t,s) = \beta$.

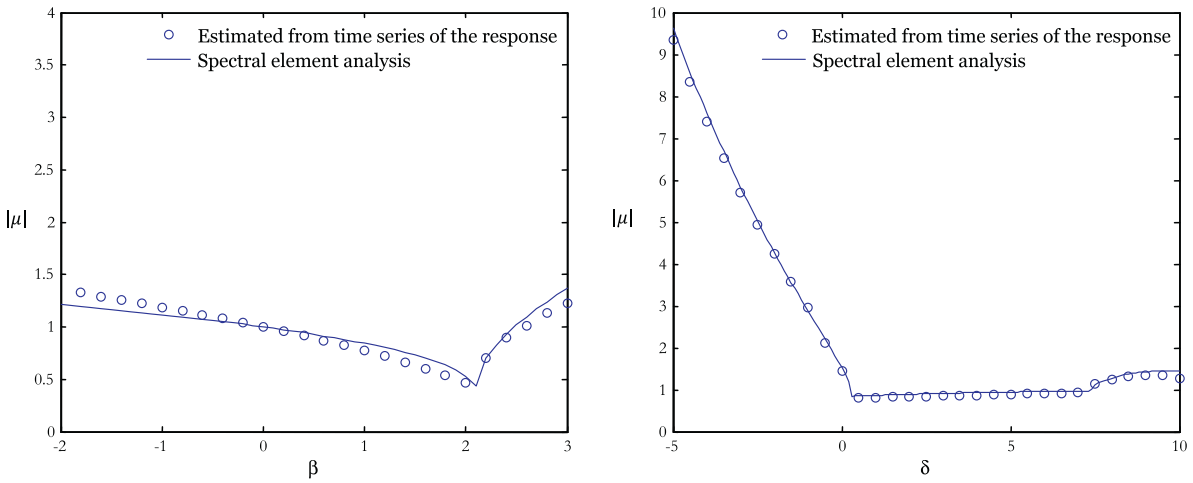

Fig. 6. Floquet multipliers estimated from time series of the response compared with the values obtained from SEA method: for $K(t,s) = \beta$, $\omega = 2\pi$, $\nu = 1$, $\epsilon = 5$, $\delta = 1.5$ and a varying β (left). Also for $K(t,s) = \beta$, $\omega = 2\pi$, $\nu = 1$, $\epsilon = 5$, $\beta = 0.8$ and a varying δ (right).

Table 3
The estimated Floquet multiplier along with the actual and identified parameters of the system.

Parameter to be identified	Estimated $\hat{\mu}$	Identified value	Actual value	Error (%)
β	0.8945	2.561	2.4	5.0
	1.007	2.527	2.6	2.8
δ	7.404	−4.155	−4.0	3.7
	2.967	−0.9299	−1.0	7.0

identification approach are listed in Table 3 along with the percentage of error. The results show that the parameter identification approach is capable of accurate parameter identification of a second order DIDE system.

The stability chart of the system in $\delta - \beta$ plane estimated from time series using the procedure described in Section 3 is compared with the stability chart obtained from SEA in Fig. 5 and the result shows an acceptable agreement.

5. Conclusions

An empirical method for parameter identification in distributed delay systems is investigated in this paper. It is shown that the Floquet multipliers of the system can be accurately estimated from the Floquet multipliers of a truncated system and the Floquet multipliers so obtained enable the identification of the unknown parameters of the system directly from experimental data.

Table A-4
The a_i coefficients of Eq. (27).

a_1	-3.9663×10^6
a_2	-1.7276×10^9
a_3	-2.5668×10^{11}
a_4	-1.5153×10^{13}
a_5	-3.6278×10^{14}
a_6	-2.7691×10^{15}
a_7	-4.3305×10^{15}

The empirical estimates for the Floquet multipliers of the system can be obtained either from the initial transients or from perturbations in the steady state motion. Floquet multipliers estimated from time series of the response are compared with the results of a recent method called spectral element analysis which is developed for stability studies of distributed delay systems. Also a dynamic map obtained using this method is used for relating the estimated Floquet multipliers to the unknown parameters of the system. The parameter identification method of this paper is successfully implemented on some numerically generated time series of the response of first and second order DIDEs and it has been shown that the approach is capable of identifying the unknown parameters accurately.

Although the examples studied in this paper are limited to DIDEs with a constant Kernel function ($K = \beta$), the approach is definitely capable of handling non-constant kernel functions $K = K(t,s)$. The additional complication would be the need to incorporate an algorithm for solving nonlinear algebraic equations. In addition, there must be data from more than one experimental run (or multiple simulations) in order to identify all the unknown parameters. The volume of the symbolic manipulation required will increase notably for non-constant kernel functions. Also note that in estimating the parameter of DIDE we assumed that the maximum delay was known, i.e. the mechanism in which the delay entered the DIDE was understood and its maximum value was known. The problem of estimating the value of the maximum delay is outside the scope of this paper but it is a topic worthy of future research.

Acknowledgement

Financial support from the National Science Foundation, under the Grant No. CMMI-0900289 is gratefully appreciated.

Appendix A

Table A-4.

References

[1] Stepan G. Delay differential equation models for machine tool chatter. In: Moon FC, editor. Dynamics and chaos in manufacturing processes. New York: Wiley; 1997. p. 165–91.
[2] Insperger T, Stepan G. "Remote control of periodic robot motion", In: Proceedings of the Thirteenth Symposium on Theory and Practice of Robots and Manipulators, Zakopane, Poland, 2000, pp. 197–203.
[3] Batzel JJ, Tran HT. Stability of the human respiratory control system I. Analysis of a two-dimensional delay state-space model. J Math Biol 2000;41:45–79.
[4] Baker CT, Bocharov GA, Paul CA, Rihan FA. Modelling and analysis of time-lags in some basic patters of cell proliferation. J Math Biol 1998;37:341–71.
[5] Szydlowski M, Krawiec A. The Kaldor–Kalecki model of business cycle as a two-dimensional dynamical system. J Nonlinear Math Phys 2001;8:266–71.
[6] Kalmar-Nagy T, Stépán G, Moon FC. Subcritical Hopf bifurcation in the delay equation model for machine tool vibrations. Nonlinear Dyn 2001;26:121–42.
[7] Epstein IR. Delay effects and differential delay equations in chemical kinetics. Int Rev Phys Chem 1992;11:135–60.
[8] Roussel MR. Approximate state-space manifolds which attract solutions of systems of delay-differential equations. J Chem Phys 1998;109:8154–60.
[9] Stépán G. Retarded dynamical systems. Harlow, UK: Longman; 1989.
[10] Stepan. Delay-differential equation models for machine tool chatter. In: Moon FC, editor. Dynamics and chaos in manufacturing processes. New York: Wiley; 1998.
[11] Khasawneh F, Mann B, Insperger T, Stepan G. Increased stability of low-speed turning through a distributed force and continuous delay model. J Comput Nonlinear Dyn 2009;4:1–12.
[12] Xie L, Fridman E, Shaked U. Robust H_∞ control of distributed delay systems with application to combustion control. IEEE Trans Automat Control 2001;46:1930–5.
[13] Takacs D, Orosz G, Stepan G. Delay effects in shimmy dynamics of wheels with stretched string-like tyres. Euro J Mech A/Solids 2009;28:516–25.
[14] Koto T. Stability of Runge–Kutta methods for delay integro-differential equations. J Comput Appl Math 2002;145:483–92.
[15] Zhang C, Vandewalle S. Stability analysis of Runge–Kutta methods for nonlinear Volterra delay-integro-differential equations. IMA J Numer Anal 2004;24:193–214.
[16] Luzyanina T, Engelborghs K, Roose D. Computing stability of differential equations with bounded distributed delays. Numer Algor 2003;34:41–66.
[17] Insperger, Stepan. Semi-discretization for time-delay systems. New York: Springer; 2011.
[18] Insperger T, Stépán G. Semi-discretization method for delayed systems. Int J Numer Methods Eng 2002;55:503–18.
[19] Khasawneh F, Mann BP. Stability of delay integro-differential equations using a spectral element method. Math Comput Model 2011;54:2493–503.
[20] Breda D, Maset S, Vermiglio R. Pseudospectral differencing methods for characteristic roots of delay differential equations. SIAM J Sci Comput 2005;27:482–95.
[21] Breda D. Solution operator approximations for characteristic roots of delay differential equations. Appl Numer Math 2006;56:305–17.

[22] Breda D, Maset S, Vermiglio R. "Numerical computation of characteristic multipliers for linear time-periodic delay differential equations", In: Proceedings of the 6th IFAC Workshop on Linear Time-Delay Systems, 2006.
[23] Bobrenkov O, Nazari M, Butcher E. Response and Stability Analysis of Periodic Delayed Systems with Discontinuous Distributed Delay. J Comput Nonlinear Dyn. 2012;7:031010 (12p).
[24] Mann BP, Young KA. An empirical approach for delayed oscillator stability and parametric identification. Proc R Soc A 2006;462:2145–60.
[25] Deshmukh V. Parametric estimation for delayed nonlinear time-varying dynamical systems. J Comput Nonlinear Dyn 2011;6. 041003-1.
[26] Khasawneh F, Mann BP. A spectral element approach for the stability of delay systems. Int J Numer Methods Eng 2011;87:566–92.
[27] Tweten DJ, Lipp GM, Khasawneh FA, Mann BP. On the comparison of semi-analytical methods for the stability analysis of delay differential equations. J Sound Vib 2012;331:4057–71.
[28] Virgin LN. Introduction to experimental nonlinear dynamics. Cambridge, UK: Cambridge University Press; 2000.
[29] Takens F. Detecting strange attractors in turbulence dynamical systems and turbulence. Springer Lect Notes Math 1981;898:366–81.
[30] Fraiser AM, Swinney HL. "Independent coordinates for strange attractor from mutual information". Phys Rev A 1986;33:1134–40.
[31] Kennel MB, Brown R, Abarbanel H. Determining embedding dimension for phase-space reconstruction using a geometrical construction. Phys Rev A 1992;45:3403–11.